Cryogenic Engineering

2017 Fall Semester

Kim, Min Soo

Chapter 7.

Cryogenic-Fluid Storage and Transfer Systems

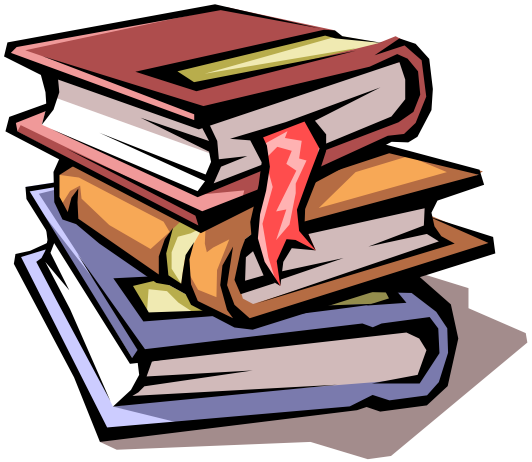

7.1 Basic Storage Vessels

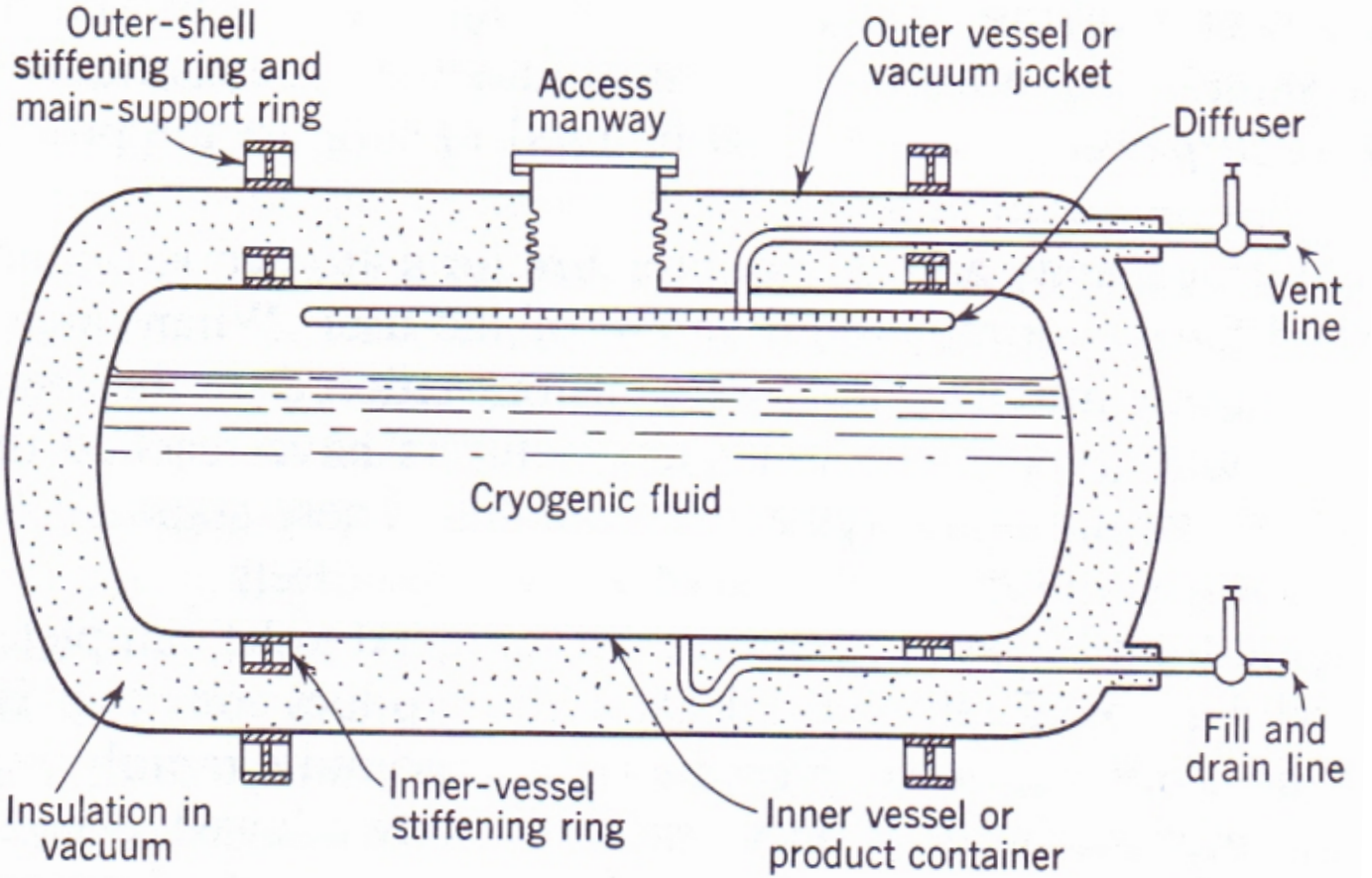

Fig. 7.1. Elements of a dewar vessel.

7.1 Basic Storage Vessels

Dewar vessel – Starting point for high-performance cryogenic fluid vessel design !

- Insulation
  - Small vessel : evacuation
  - Large vessel : powders, fibrous materials, multi-layer insulation
- Vapor vent line : Vapor escape due to heat inleak
- Liquid removal : pressurization with warm gas, liquid pump

※ Storage vessel filling ~90%

① Heat inleak – vaporization

② Prevention of liquid from flowing through the vent tube

7.2 Inner-vessel design

The minimum thickness of the inner shell for a cylindrical vessel

$$t = \frac{pD}{2s_a e_w - 1.2p} = \frac{pD_o}{2s_a e_w + 0.8p}$$

The minimum thickness for spherical shells, hemispherical heads or ASME torispherical heads

$$t = \frac{pDK}{2s_a e_w - 0.2p} = \frac{pD_o K}{2s_a e_w + 2p(K - 0.1)} \qquad K = \frac{1}{6}\left[2 + \left(\frac{D}{D_1}\right)^2\right]$$

p = design internal pressure (absolute pressure for vacuum-jacketed vessels)
D = inside diameter of shell
D_o = outside diameter of shell
s_a = allowable stress (approximately one-forth minimum ultimate strength of material)
e_w = weld efficiency
D_1 = minor diameter of the elliptical head

7.2 Inner-vessel design

Table 7.1. Allowable stress for materials at room temperature or lower (ASME Code, Section VIII, 1983)

Material		Allowable Stress MPa	Allowable Stress psi
Carbon steel (for outer shell only)	SA-285 Grade C	94.8	13 750
	SA-299	129.2	18 750
	SA-442 Grade 55	94.8	13 750
	SA-516 Grade 60	103.4	15 000
Low-alloy steel	SA-202 Grade B	146.5	21 250
	SA-353-B (9% Ni)	163.7	23 750
	SA-203 Grade E	120.6	17 500
	SA-410	103.4	15 000
Stainless steel	SA-240 (304)	129.2	18 750
	SA-240 (304L)	120.6	17 500
	SA-240 (316)	129.2	18 750
	SA-240 (410)	112.0	16 250
Aluminum	SB-209 (1100-0)	16.2	2 350
	SB-209 (3004-0)	37.9	5 500
	SB-209 (5083-0)	68.9	10 000
	SB-209 (6061-T4)	41.4	6 000
Copper	SB-11	46.2	6 700
	SB-169 (annealed)	86.2	12 500
Nickel alloys (annealed)	SB-127 (Monel)	128.2	18 600
	SB-168	137.9	20 000

Table 7.2. Weld efficiencies for arc-welded and gas-welded joints (ASME Code, Section VIII, 1983)

Type of Joint	Fully Radiographed	Spot Examined	Not Spot Examined
Butt joints with complete penetration	1.00	0.85	0.70
Single-welded butt joint, backing strip	0.90	0.80	0.65
Single-welded butt joint, no backing strip	...	...	0.60
Double full-fillet lap joint	...	...	0.55

7.2 Inner-vessel design

- **The bending-moment expression**

$$0 \le \phi \le \theta \longrightarrow \frac{2\pi M}{WR} = 0.5\cos\phi + \phi\sin\phi - (\pi - \theta)\sin\theta + \cos\theta + \cos\phi\sin^2\theta$$

$$0 \le \phi \le \pi \longrightarrow \frac{2\pi M}{WR} = 0.5\cos\phi - (\pi - \phi)\sin\phi + \theta sin\theta + cos\theta + cos\phi sin^2\theta$$

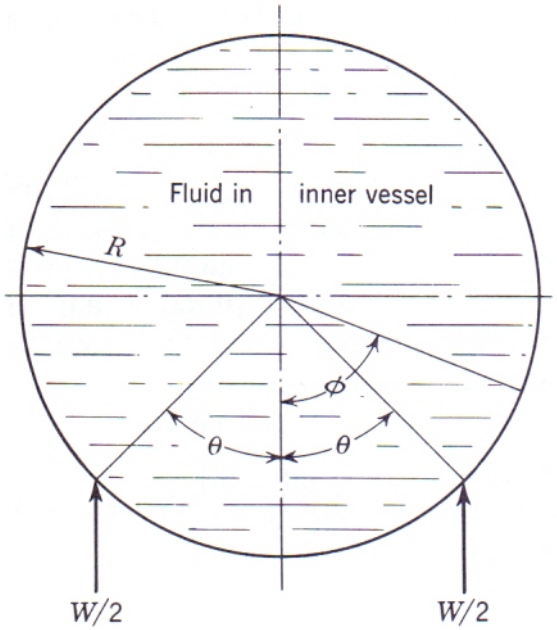

M = bending moment

W = weight of fluid supported by the stiffening ring

R = mean radius of the ring

Fig. 7.2. Loading on the inner-shell stiffening ring.

7.3 Outer-vessel design

Table 7.5. Typical mechanical properties of metals

Metal	Density		Young's Modulus		Poisson's Ratio
	kg/m^3	lb_m/in^3	GPa	psi	
Carbon steel	7720	0.279	200	29×10^6	0.27
Low-alloy steel	7830	0.283	200	29×10^6	0.27
Stainless steel	7920	0.286	207	30×10^6	0.28
Aluminum	2700	0.098	69	10×10^6	0.33
Copper	8940	0.323	117	17×10^6	0.33
Monel	8830	0.319	179	26×10^6	0.32

7.3 Outer-vessel design

The collapsing or critical pressure for a long cylinder exposed to external pressure

$$p_c = \frac{2E(t/D_o)^3}{1-v^2}$$

$E =$ Young's modulus of shell material

$t =$ Shell thickness

$D_o =$ Outside diameter of shell

$v =$ Poisson's ratio for shell material

The collapsing pressure for a short cylinder subjected to external pressure

$$p_c = \frac{2.42E(t/D_o)^{5/2}}{(1-v^2)^{3/4}[(L/D_o) - 0.45(t/D_o)^{1/2}]}$$

7.3 Outer-vessel design

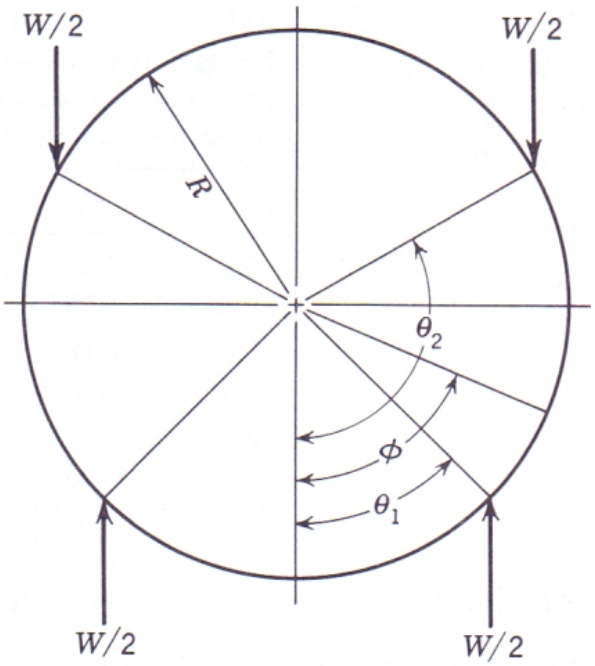

Fig. 7.4. Loading on the outer-shell support ring due to the weight of the inner vessel and contents.

1. For $0 \le \phi \le \theta_1$

$$2\pi M/W R = \cos\phi(\sin^2\theta_2 - \sin^2\theta_1) + (\cos\theta_2 - \cos\theta_1) - (\pi - \theta_2)\sin\theta_2 + (\pi - \theta_1)\sin\theta_1$$

2. For $\theta_1 \le \phi \le \theta_2$

$$2\pi M/W R = \cos\phi(\sin^2\theta_2 - \sin^2\theta_1) + (\cos\theta_2 - \cos\theta_1) - (\pi - \theta_2)\sin\theta_2 + \pi\sin\phi - \theta_1\sin\theta_1$$

3. For $\theta_2 \le \phi \le \pi$

$$2\pi M/W R = \cos\phi(\sin^2\theta_2 - \sin^2\theta_1) + (\cos\theta_2 - \cos\theta_1) + (\theta_2\sin\theta_2 - \theta_1\sin\theta_1)$$

7.3 Outer-vessel design

Fig. 7.5. Bending moment curve for the outer-shell support ring. The location angle ϕ and support angles θ_1 and θ_2 are defined in Fig. 7.4.

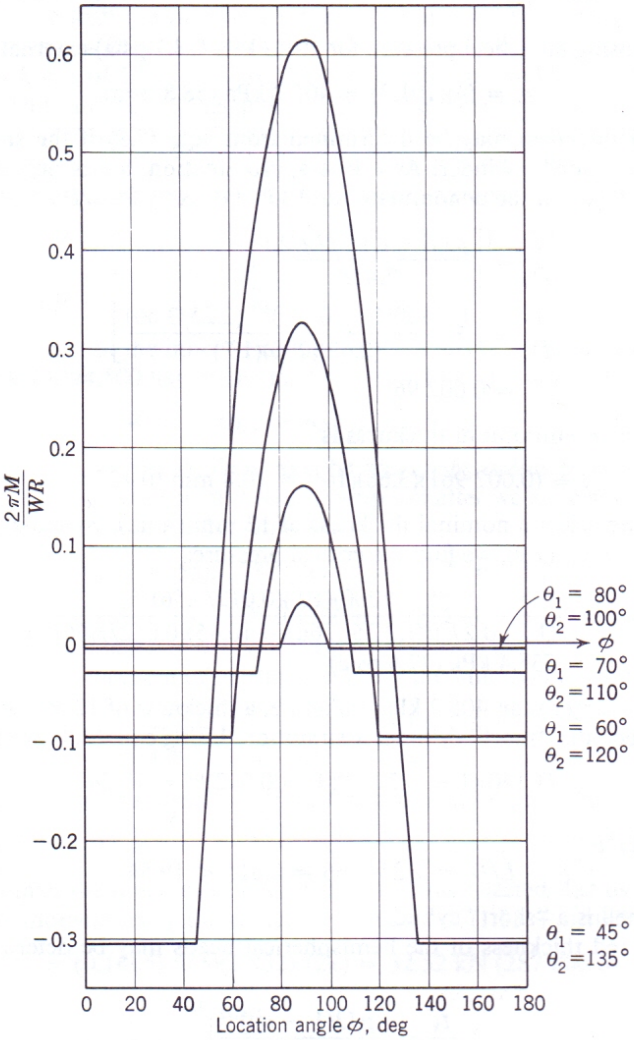

7.4 Suspension system design

Fig. 7.7. Typical methods of supporting the inner vessel within the outer vessel in a dewar.

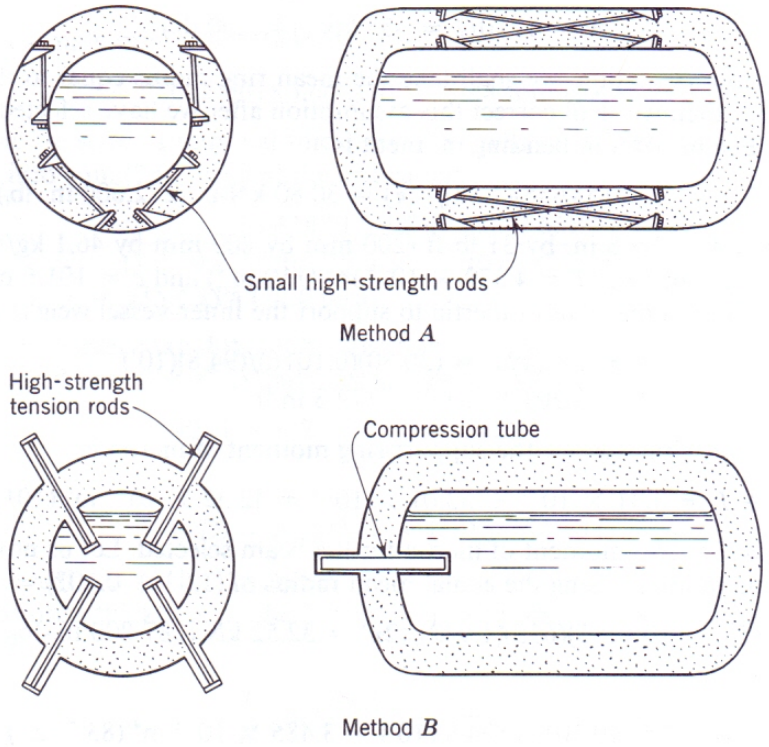

Table 7.7. Acceleration loads specified in suspension system design for cryogenic-fluid storage vessels

Type of unit	Vertical Up, g	Vertical Down, g	Transverse, g	Longitudinal g
Stationary storage vessels:				
Empty	0.5	3	0.5	5
Full	0.5	1.5	0.5	0.5
Full with blast loading	3	5	4	4
Transport trailers:				
Small (below 4 m^3 or 1060 gal U.S.)	2	5	4	8
Large (above 4 m^3)	1	4	2	4

7.4 Suspension system design

Fig. 7.8. Dynamic loading conditions for support system shown in Fig. 7.7*a*.

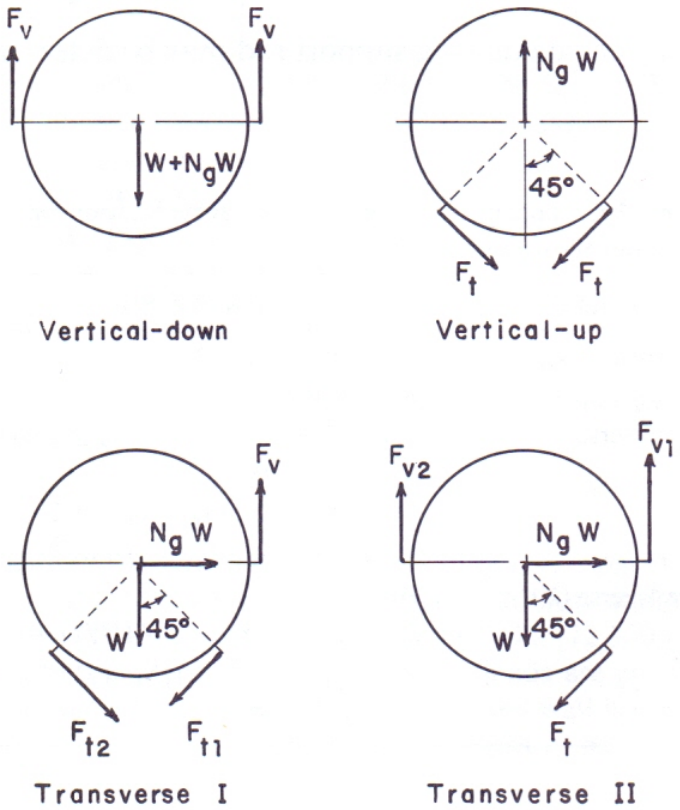

Table 7.8. Forces in the vertical and transverse rods for the cases shown in Fig. 7.8

Loading	Force in Rods
Vertical-down	$F_v = (1 + N_g)W/2$
Vertical-up	$F_t = N_g W/\sqrt{2}$
Transverse (I)	For $(\sqrt{2} - 1)N_g \geqq 1$ or $N_g \geqq 2.414$
	$F_v = \sqrt{2}\, N_g W$
	$F_{t1} = [(\sqrt{2} + 1)N_g - 1]W/\sqrt{2}$
	$F_{t2} = [(\sqrt{2} - 1)N_g - 1]W/\sqrt{2}$
Transverse (II)	For $N_g < 2.414$
	$F_{v1} = [1 + (\sqrt{2} + 1)N_g]W/2$
	$F_{v2} = [1 - (\sqrt{2} - 1)N_g]W/2$
	$F_t = \sqrt{2}\, N_g W$

$$2F_v - W - N_g W = 0$$

$$F_v = \left(1 + N_g\right) W/2$$

$N_g =$ Acceleration load

$W =$ Weight of the inner vessel and its contents

7.4 Suspension system design

- **The heat-transfer rate down a support rod**

$$\dot{Q} = \frac{k_m A(T_h - T_c)}{L} = (K_h - K_c)\left(\frac{A}{L}\right)$$

$k_m =$ Mean thermal conductivity of rod $= (K_h - K_c)/(T_h - T_c)$

$T_h =$ Temperature of the warm end of the rod

$T_c =$ Temperature of the cold end of the rod

$A =$ Cross-sectional area of the rod

$L =$ Length of the rod

$K = \int_{4K}^{T} k_t dT =$ Thermal conductivity integral

7.5 Piping

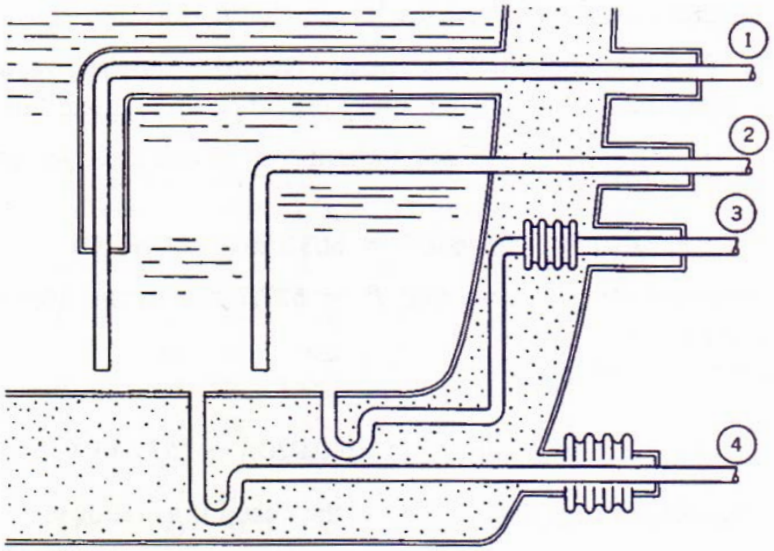

Fig. 7.10. Cryogenic-fluid storage-vessel piping arrangements.

The minimum wall thickness for piping subjected to internal pressure

$$t = \frac{pD_o}{2s_a + 0.8p}$$

$p =$ Design pressure

$D_o =$ Outside diameter of pipe

$s_a =$ Allowable stress of pipe material

7.6 Draining the vessel

- In order to force the liquid from the inner vessel :

① Self-pressurization of the inner vessel

② External gas pressurization

③ Pump transfer

7.7. Safety devices

The basic minimum safety devices
used on larger cryogenic-fluid storage vessels include:

(1) The inner-vessel pressure-relief valve
(2) The inner-shell burst-disc assembly
(3) The annular-space burst-disc assembly

The required size of the safety valve

$$A_v = \dot{m}_g \, (R_u \, T / g_c \, M)^{1/2} / C \, K_D p_{\max}$$

$A_v =$ Discharge area of valve

$\dot{m}_g =$ Maximum mass flow rate through valve

$R_u =$ Universal gas constant

$T =$ Absolute temperature of the gas at the inlet to the valve

$M =$ Molecular weight of gas flowing through the valve

$g_c =$ Unit conversion factor in Newton's Second Law

$K_D =$ Discharge coefficient determined by test

$p_{\max} =$ (set gauge pressure)(1.1)+(atmospheric pressure)

$\gamma = c_p / c_v =$ Specific heat ratio of gas

$$C = \left[\gamma \left(\frac{2}{\gamma + 1} \right)^{(\gamma+1)/(\gamma-1)} \right]^{1/2}$$

7.7. Safety devices

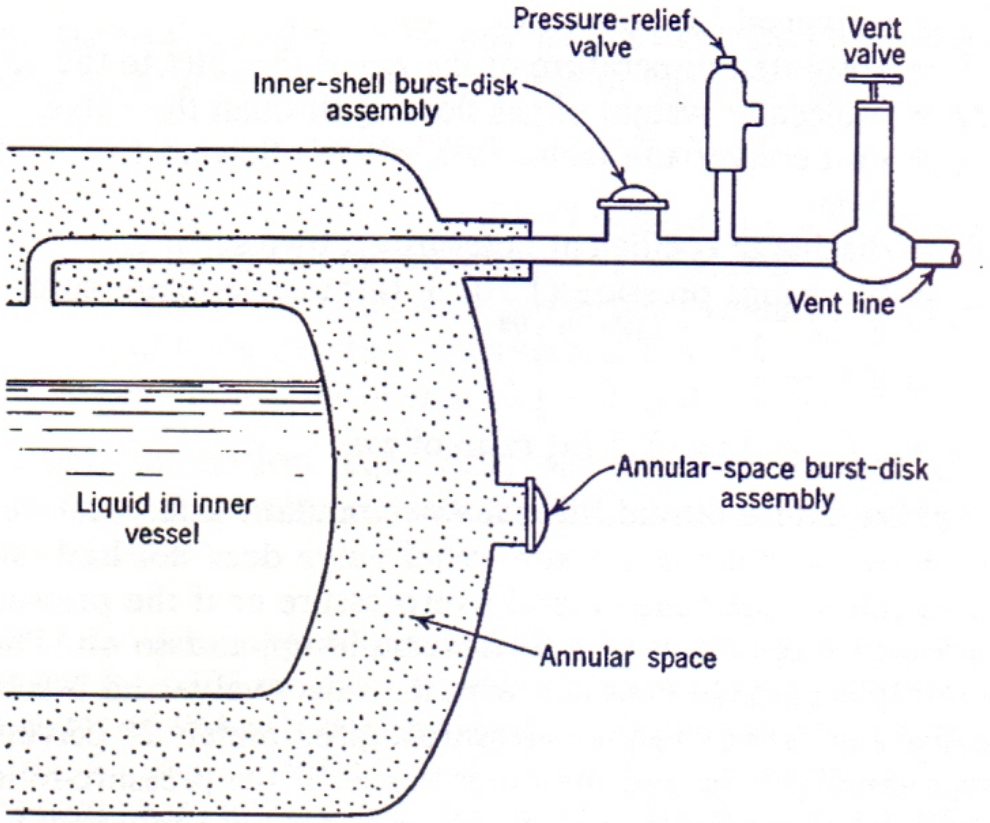

Fig. 7.11. Location of basic safety devices in a dewar. Note that the inner-shell burst-disk assembly and pressure-relief valve are located *between* the inner vessel and the vent valve.

7.7. Safety devices

There are several types of insulation that can be used in cryogenic equipment.

(1) Expanded foams

(2) Gas-filled powders and fibrous materials

(3) Vacuum alone

(4) Evacuated powders and fibrous materials

(5) Opacified powders

(6) Multilayer insulations

7.8 Expanded-foam insulations

Table 7.12. Apparent thermal conductivity of foam insulations for boundary temperatures of 300 K (80°F) and 77 K (−139°F)

	Density		Thermal Conductivity	
Foam	kg/m^3	lb_m/ft^3	mW/m-K	Btu/hr-ft-°F
Polyurethane	11	0.70	33	0.019
Polystyrene	39	2.4	33	0.019
	46	2.9	26	0.015
Rubber	80	5.0	36	0.021
Silica	160	10.0	55	0.032
Glass	140	8.7	35	0.020

7.9 Gas filled powders and fibrous insulations

Component of porous insulations :

fiber glass, powdered cork, perlite, Santocel, rock wool, and Vermiculite

Table 7.13. Apparent thermal conductivity of gas-filled powders and fibrous insulations for boundary temperatures of 300 K (80°F) and 90 K (−298°F)

	Density		Thermal Conductivity	
Insulation	kg/m^3	lb_m/ft^3	mW/m-K	Btu/hr-ft-°F
Perlite	50	3.1	26	0.015
	210	13.1	44	0.025
Silica aerogel	80	5.0	19	0.011
Vermiculite	120	7.5	52	0.030
Fiber glass	110	6.9	25	0.014
Rock wool	160	10.0	35	0.020

7.10 Vacuum insulation

Vaccum insulation essentially eliminates two components of heat transfer: solid conduction, and gaseous convection, which means that only **radiant heat transfer** remains

radiant heat transfer: $\dot{Q} = F_e F_{1-2} \sigma A_1 (T_2^4 - T_1^4)$

$F_e =$ Emissivity factor

$F_{1-2} =$ Configuration factor (=1)

$\sigma =$ Stefan-Boltzman constant

$T =$ absolute temperature

7.10 Vacuum insulation

The emissivity factor for diffuse radiation for concentric or cylinders is given by:

$$\frac{1}{F_e} = \frac{1}{e_2} + \frac{A_1}{A_2}\left(\frac{1}{e_1} - 1\right)$$

7.10 Vacuum insulation

For N shields between the hot and cold surfaces, the emissivity factor for a shield emissivity e_s is:

$$\frac{1}{F_e} = \left(\frac{1}{e_1} + \frac{1}{e_s} - 1\right) + (N-1)\left(\frac{1}{e_2} - 1\right) + \left(\frac{1}{e_2} + \frac{1}{e_s} - 1\right)$$

As an example of the effectiveness of radiation shields, suppose we consider a pair of surfaces having an emissivity $e_1 = e_2 = 0.8$. For parallel flat plates, we obtain

$$F_e(no\ shelds) = 0.6667 \qquad F_e(10\ shelds) = 0.00255$$

7.10 Vacuum insulation

To deficit the simple conduction model, consider gas molecules between two parallel plates with constant temperatures, transferring energy from high to low temperature side.

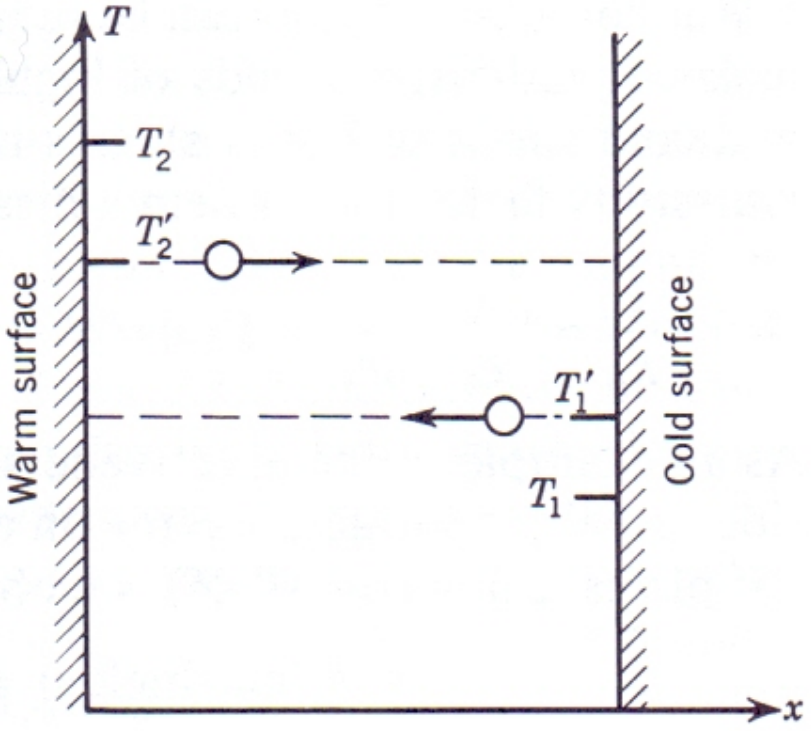

Fig. 7.12. Energy transport and molecule "temperature" for free-molecular conduction.

7.10 Vacuum insulation

The degree of approach of the molecules to thermal equilibrium upon collision is expressed by the accommodation coefficient, defined by

$$a = \frac{actual\ energy\ transfer}{maximum\ possible\ energy\ transfer}$$

Cold surface, $a_1 = \frac{T_2' - T_1'}{T_2' - T_1}$ Hot surface, $a_2 = \frac{T_2' - T_1'}{T_2 - T_1'}$

7.10 Vacuum insulation

Solving for the temperature difference between the warm and cold surfaces, we obtain

$$T_2 - T_1 = \left(\frac{1}{a_1} + \frac{1}{a_2} - 1\right)(T_2' - T_1') = \frac{T_2' - T_1'}{e_2}$$

The accommodation coefficient factor is given by

$$\frac{1}{F_a} = \frac{1}{a_1} + \frac{A_1}{A_2}\left(\frac{1}{a_2} - 1\right)$$

7.10 Vacuum insulation

Total change in energy per unit mass of the molecules striking the wall is sum of the change in internal energy plus the change in kinetic energy of the molecules moving perpendicular to the surface. Thus,

$$\Delta e = (c_v + \frac{1}{2}R)(T_2' - T_1')$$

Eliminating the effective molecule temperatures in terms of the surface temperatures, we obtain

$$\Delta e = \frac{1}{2}F_a R(T_2 - T_1)\frac{\gamma + 1}{\gamma - 1}$$

7.10 Vacuum insulation

The energy transfer rate by molecular conduction may now be determined:

$$\frac{\dot{Q}}{A} = \frac{\dot{m}}{A}\Delta e \longrightarrow \frac{\dot{Q}}{A} = GpA_1(T_2 - T_1)$$

7.11 Evacuated powder and fibrous insulation

- One obvious method of reducing the heat transfer rate through these insulations is to evacuate the gas from the insulation

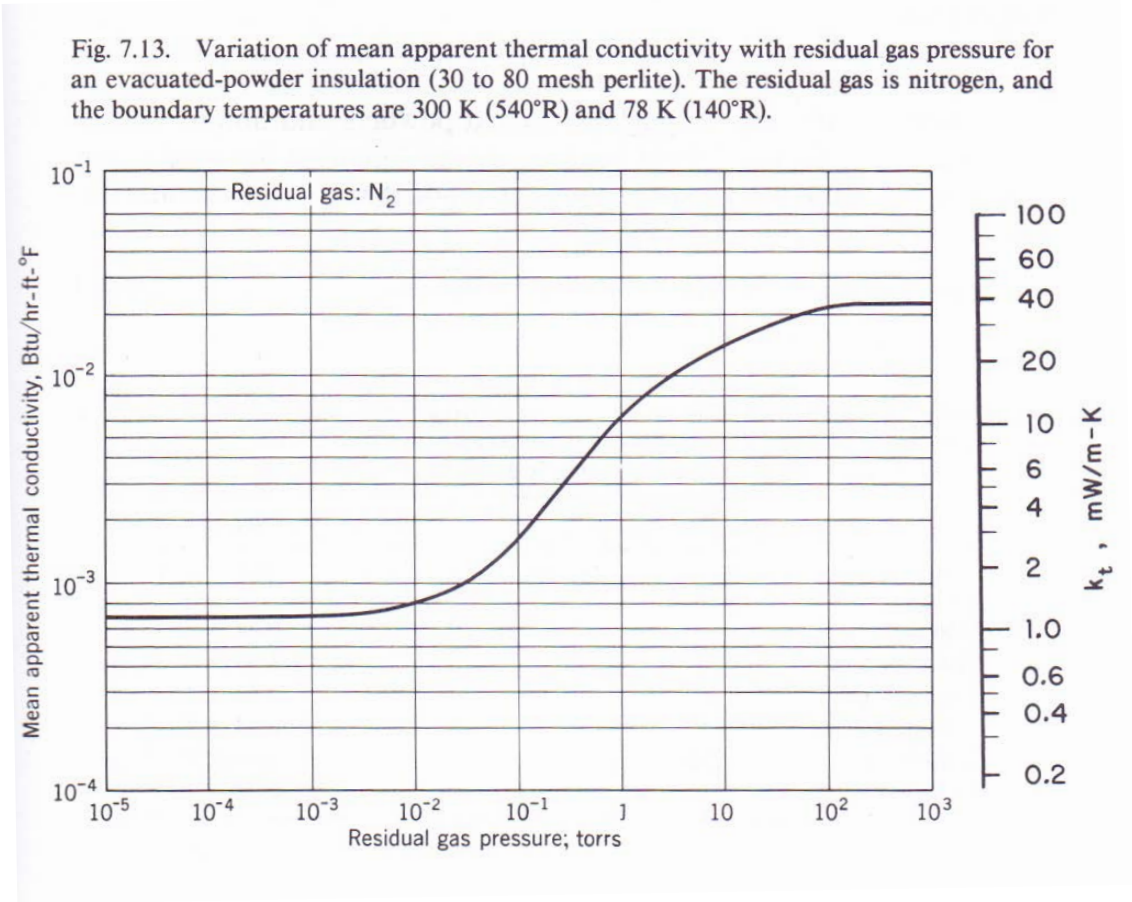

Fig. 7.13. Variation of mean apparent thermal conductivity with residual gas pressure for an evacuated-powder insulation (30 to 80 mesh perlite). The residual gas is nitrogen, and the boundary temperatures are 300 K (540°R) and 78 K (140°R).

7.11 Evacuated powder and fibrous insulation

- Temperature between ambient and liquid

  → Evacuated powders are superior compared with vacuum alone

- Temperature between LN_2 and LH_2 or LHe temperature

  → using vacuum alone is more advantageous

7.12 Opacified powder insulations

The insulation performance could be improved by any method that reduces radiant heat transfer. This improvement in performance has been accomplished by the addition of copper or aluminum flakes to evacuated powders.

Fig. 7.14. Variation of thermal conductivity with percent opacifier for opacified-powder insulations (Riede and Wang 1960).

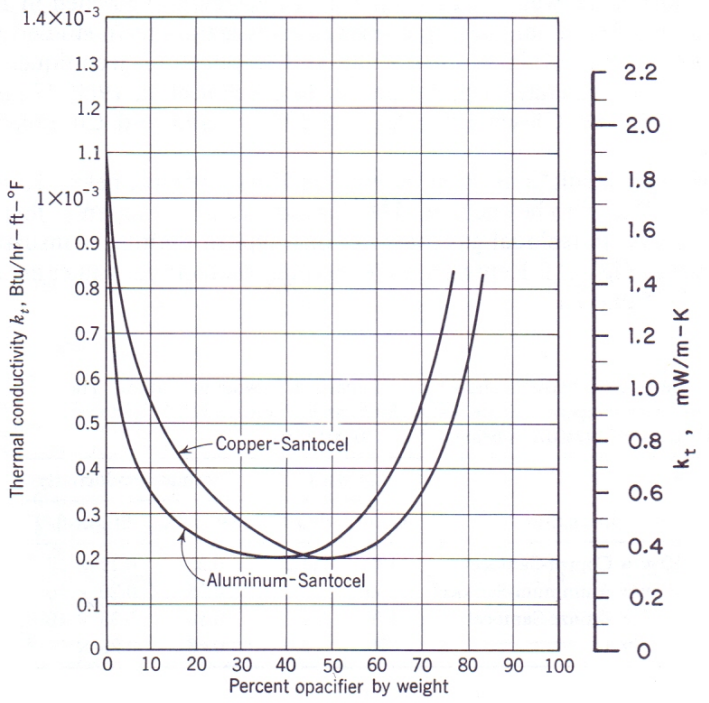

7.12 Opacified powder insulations

- Advantages : Lower thermal conductivity at appropriate opacifier percent
- Disadvantages : Vibration could cause packing of the metal flakes, which increases thermal conductivity of the powders

7.13 Multilayer insulations

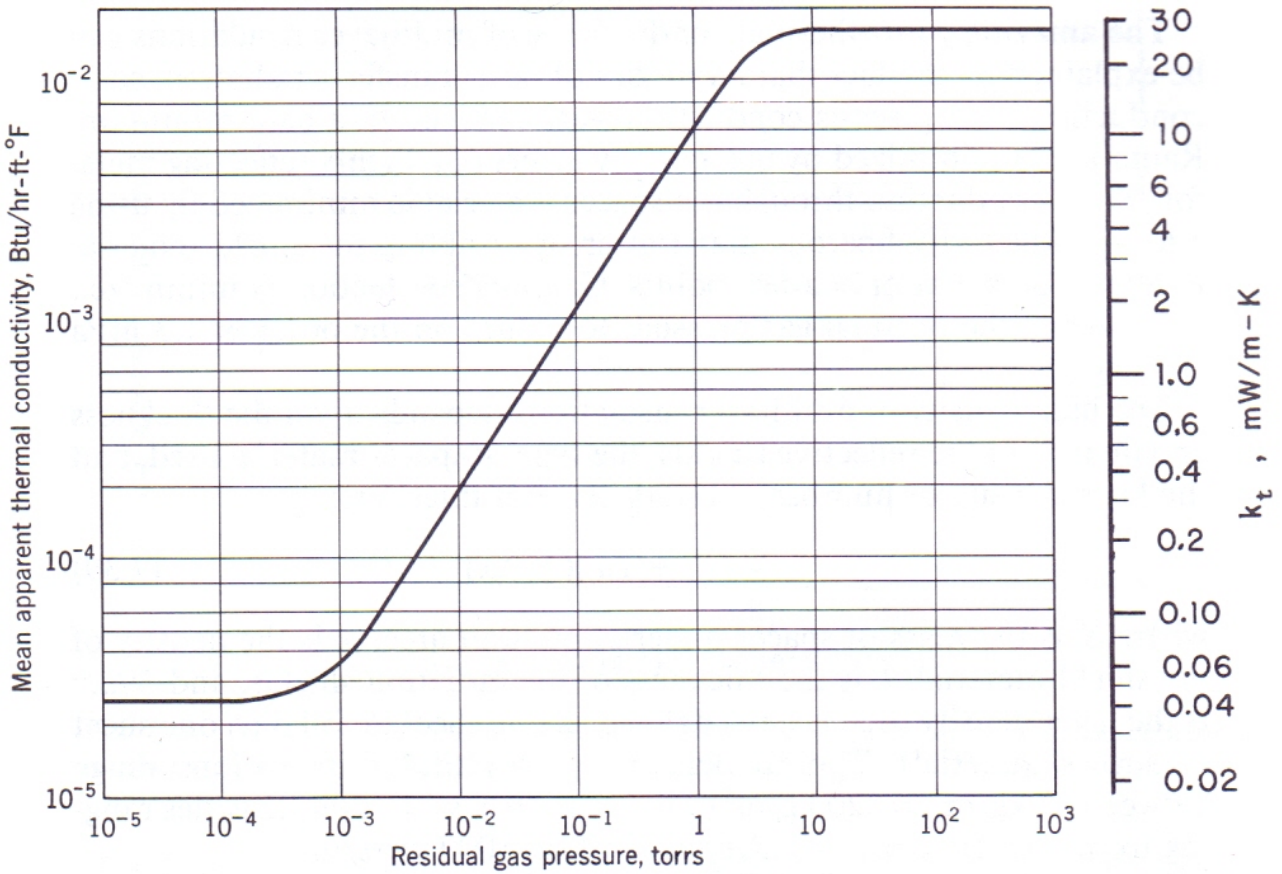

Fig. 7.15. Variation of mean apparent thermal conductivity with residual gas pressure for a typical multilayer insulation. The insulation layer-density is 24 layers/cm (60 layers/in.), and the boundary temperatures are 300 K (540°R) and 90.5 K (163°R).

7.13 Multilayer insulations

Multilayer insulations consist of **alternating layers of a highly reflecting material**, such as aluminum foil, copper foil, or aluminized Mylar, and a low conductivity spacer. Multilayer insulations must be evacuated to pressures below 10mPa to be effective.

Table 7.17. Thermal conductivity for multilayer insulations for boundary temperatures of 300 K (80°F) and 77.4 K (−321°F) with residual gas pressures of 1.3 mPa (10^{-5} torr)

Insulation	Layer Density		Thermal Conductivity	
	layer/cm	layer/in.	μW/m-K	Btu/hr-ft-°F
0.006-mm aluminum foil + 0.15-mm Fiberglass paper	20	50	37	2.1×10^{-5}
0.006-mm aluminum foil + 2-mm mesh rayon net	10	25	78	4.5×10^{-5}
0.006-mm aluminum foil + 2-mm mesh nylon net	11	28	34	2.0×10^{-5}
NRC-2 crinkled aluminized Mylar film 0.006 mm	35	89	42	2.4×10^{-5}
Dimplar dimpled + smooth Mylar film	8	20	42	2.4×10^{-5}
0.0087-mm aluminum foil + carbon-loaded glass-fiber paper[a]	30	76	14	0.85×10^{-5}

[a]Residual gas pressure = 0.4 mPa = 3×10^{-6} torr

7.13 Multilayer insulations

Bulk density of multilayer insulations becomes,

$$\rho_a = (S_s + \rho_r t_r)(N/\Delta x)$$

S_s: mass of spacer material per unit area

ρ_r: density of the shield material

t_r: thickness of the radiation shields

$N/\Delta x$: the layer density

7.13 Multilayer insulations

For a well evacuated multilayer insulation, the apparent thermal conductivity may be determined from

$$k_t = (N/\Delta x)^{-1}[h_c + \sigma e(T_h^2 + T_c^2)(T_h + T_C)/(2 - e)$$

σ: Stefan-Boltzmann constant

e: effective emissivity of the shield material

T: boundary temperatures

7.13 Multilayer insulations

Relation of thermal conductivity with Layer density is represented as below

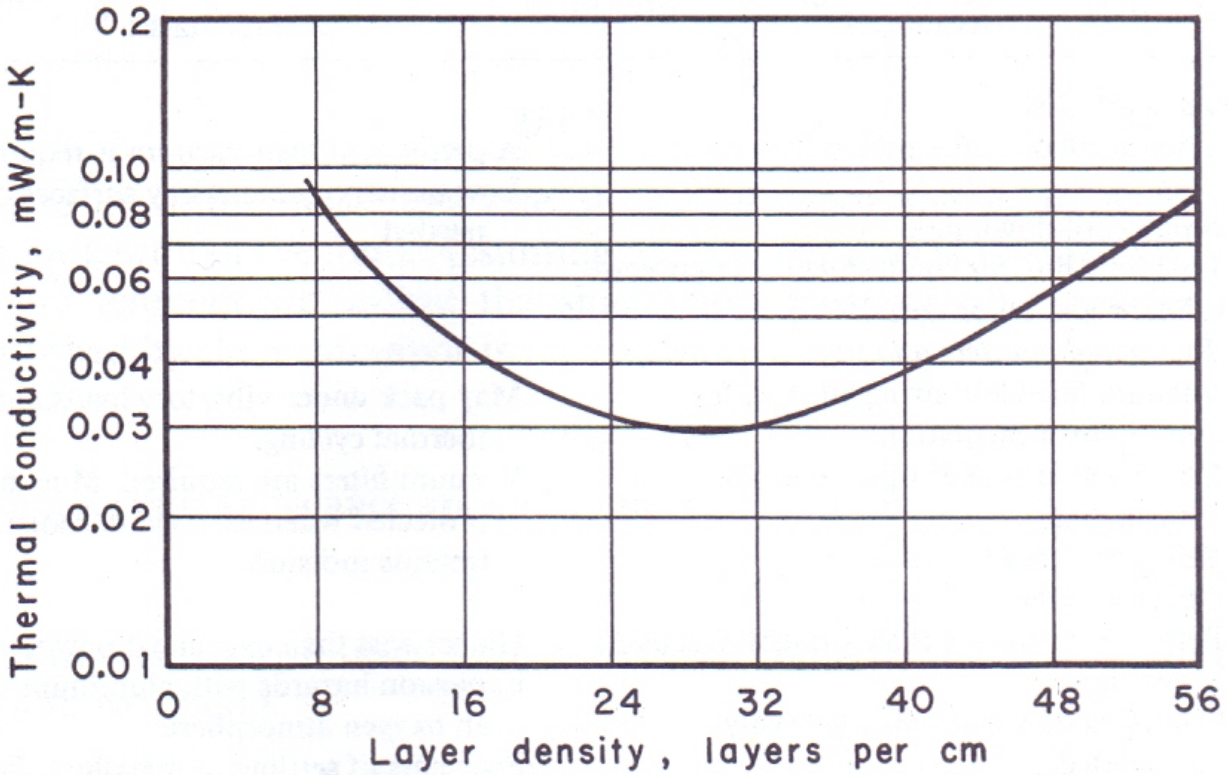

Fig. 7.16. Variation of thermal conductivity with layer density for a typical multilayer insulation (Wang 1961). The boundary temperatures are 294 K (530°R) and 78 K (140°R).

7.14 Comparison of insulations

- A comparison of the advantages and disadvantages of the insulations

	Advantages	Disadvantages
1. Expanded foams	Low cost No need for rigid vacuum jacket Good mechanical strength	High thermal contraction Conductivity may change with time
2. Gas-filled powders a nd fiberous materials	Low cost Easily applied to irregular shapes Not flammable	Vapor barrier is required Powder can pack Conductivity is increased
3. Vacuum alone	Complicated shapes may be easily insulated Small cool-down loss Low heat flux for small thickness between inner and outer vessel	A permenent high vacuum is required Low-emissivity boundary surfaces needed

7.14 Comparison of insulations

- A comparison of the advantages and disadvantages of the insulations

	Advantages	Disadvantages
4. Evacuated powders and fibrous materials	Vacuum level less stringent than for multilayer insulations Complicated shapes may be easily insulated Relatively easy to evacuate	May pack under vibratory loads and thermal cycling Vacuum filters are required. Must be protected when exposed to moist air (retains moisture)
5. Opacified powders	Better performance than straight evacuated powders Complicated shapes may be easily insulated Vacuum requirement is not as stringent as for multilayer insulations and vacuum alone	Higher cost than evacuated powders Explosion hazards with aluminum in an oxygen atmosphere Problems of settling of metallic flakes
6. Multilayer insulations	Best performance of all insulations Low weight Lower cool-down loss compared with powders Better stability than powders	High cost per unit volume Difficult to apply to complicated shapes Problems with lateral conduction More stringent vacuum requirements than powders

7.15 Vapor-shielded vessels

Another method of reducing the heat inleak
→ use the cold vent gas to refrigerate an intermediate shield

Fig. 7.17. Vapor-shielded cryogenic-fluid storage vessel.

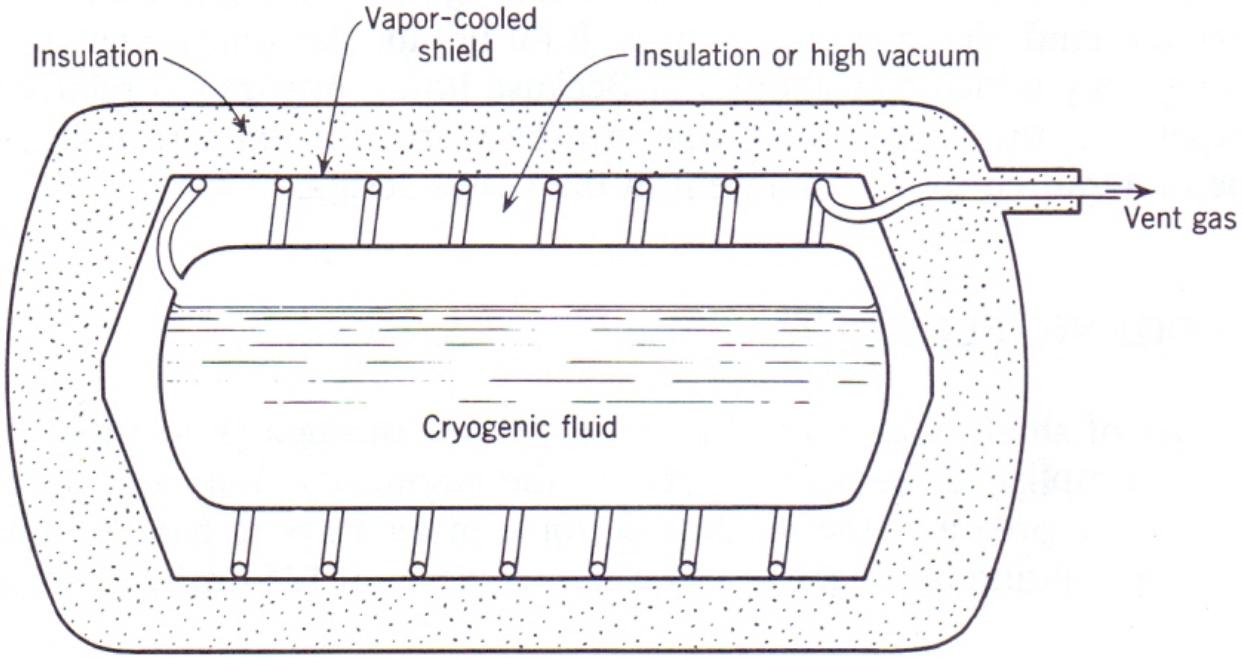

7.15 Vapor-shielded vessels

The effectiveness depends upon
the ratio of sensible heat absorbed by the vent gas to the latent heat of the fluid

The heat transfer rate from ambient to the vapor shield through all paths :

$$\dot{Q}_{2-s} = U_2(T_2 - T_s) = U_2[(T_2 - T_1) - (T_s - T_1)]$$

$$U_2 = \left(\frac{k_t A}{\Delta x}\right)_{ins} + \left(\frac{k_t A}{\Delta x}\right)_{sup} + \left(\frac{k_t A}{\Delta x}\right)_{piping}$$

K_t : thermal conductivity for the insulation, supports, piping
A : heat-transfer area for each of these components
Δx : the length of conduction path

7.15 Vapor-shielded vessels

The heat transfer rate between the sheild and the product container :

$$\dot{Q}_{s-1} = U_1(T_s - T_1) = \dot{m}_g h_{fg}$$

$\dot{m}_g$: mass flow rate of boil-off vapor

h_{fg} : the heat of vaporization of the fluid

Assuming that the vent gas is warmed up to the shield temperature within the shiled flow passage,

The sensible heat absorbed by the vent vapor is :

$$\dot{Q}_g = \dot{m}_g C_p(T_s - T_1) \qquad \dot{Q}_{2-s} = \dot{Q}_{s-1} + \dot{Q}_g$$

7.15 Vapor-shielded vessels

From an energy balance,

$$\dot{Q}_{2-s} = \dot{Q}_{s-1} + \dot{Q}_g$$

$$U_2[(T_2 - T_1) - (T_s - T_1)] = U_1(T_s - T_1) + U_1 C_p (T_s - T_1)^2 / h_{fg}$$

By Introducing the following dimensionless parameters,

$$\pi_1 = C_p(T_2 - T_1)/h_{fg}$$
$$\pi_2 = U_1/U_2$$
$$\theta = (T_s - T_1)/(T_2 - T_1)$$

$$\pi_1 \pi_2 \theta^2 + (\pi_2 + 1)\theta - 1 = 0$$

$$\theta = \frac{\pi_2 + 1}{2\pi_1 \pi_2}\left\{\left[1 + \frac{4\pi_1 \pi_2}{(\pi_2 + 1)^2}\right]^{\frac{1}{2}} - 1\right\}$$

7.15 Vapor-shielded vessels

The variation of the shield temperature with π_2 for selected π_1

→ Shield temperature is greatest for the larger values of sensible to latent heat.

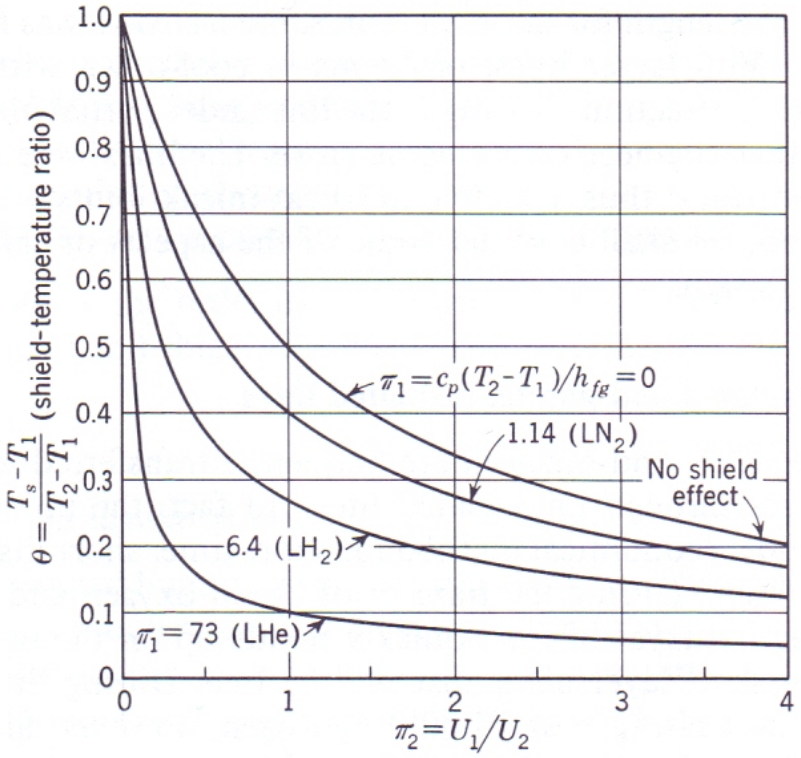

Fig. 7.18. Variation of the shield temperature ratio with conductance ratio for a vapor-shielded cryogenic-fluid storage vessel.

7.15 Vapor-shielded vessels

If the mass flow rate through the shield were zero, the shield temperature would be

$$\theta_0 = 1/(\pi_2 + 1),$$

The ratio of heat inleak with vapor shielding to heat inleak without vapor shielding would be

$$\frac{\dot{Q}}{\dot{Q}_0} = \frac{\theta}{\theta_0}$$

Fig. 7.19. Variation of the heat-inleak ratio (heat inleak with vapor shielding/heat inleak with no shield) with conductance ratio for a vapor-shielded cryogenic-fluid storage vessel.

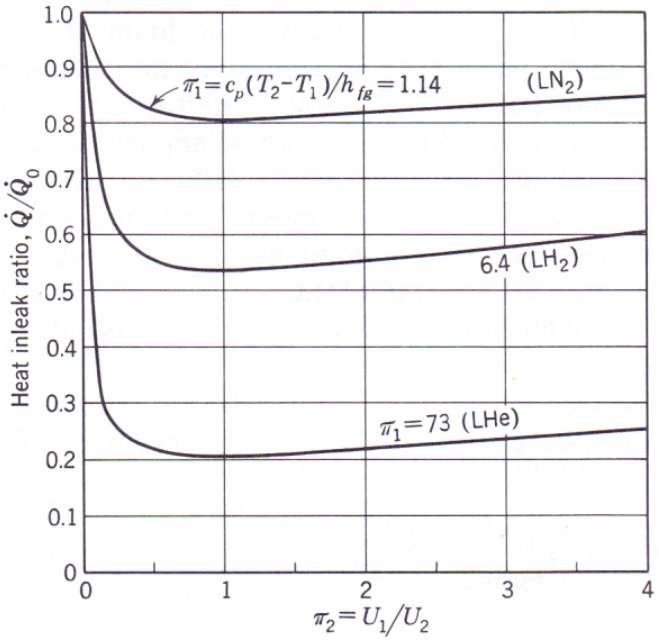

7.16 Uninsulated and porous-insulated lines

Liquid O_2, Liquid N_2 (Pressurized) :

A layer of frost quickly builds up on the outside of the line,
and this frost layer helps insulate the line.

The heat flux to liquid-O_2 line : 1.8 kW/㎡ (initally)
→ 1.0 kW/㎡ (after a 2.5mm layer of frost has formed)
→ 2.8 kW/㎡ (with a 3.6m/s wind blowing across)

Liquid H_2, Liquid N_2(Subcooled) :

Air condenses on the outside of the line,
and this causes an increased heat-transfer rate. (The latent heat is transferred)
Liquid air also tends to wash away some of the frost that is formed initially.

The heat flux for liquid-H_2 line : 11 kW/㎡ (for still air around the line)
~19 kW/㎡ (for 6.7m/s wind blowing across)

7.16 Uninsulated and porous-insulated lines

If no air condensation is present within the insulation,
the steady-state heat transfer to a porous-insulated line

$$\dot{Q} = \frac{A_0(T_a - T_f)}{\frac{D_0 \ln\left(\frac{D_0}{D_i}\right)}{2k_t} + \frac{1}{h_0}}$$

A_0 : outside surface area of the insulation ($= \pi D_0 L$)
D_0, D_i : outside and inside diameters of insulation layer
T_a : ambient temperature
T_f : fluid temperature
k_t : insulation thermal conductivity
h_0 : convection coefficient on outside of insulation

7.17 Vacuum-insulated lines

Inner line : withstand the internal pressure
Outer vacumm jacket : support the collapsing load of atmospheric pressure

"The thermal-contraction problem"
The disadvantages in placing the expansion bellows in the inner line
→ If a leak develops in the bellows,
an additional pressure drop would be introduced (Because of vacuum space!)

∴ Use U-bends!

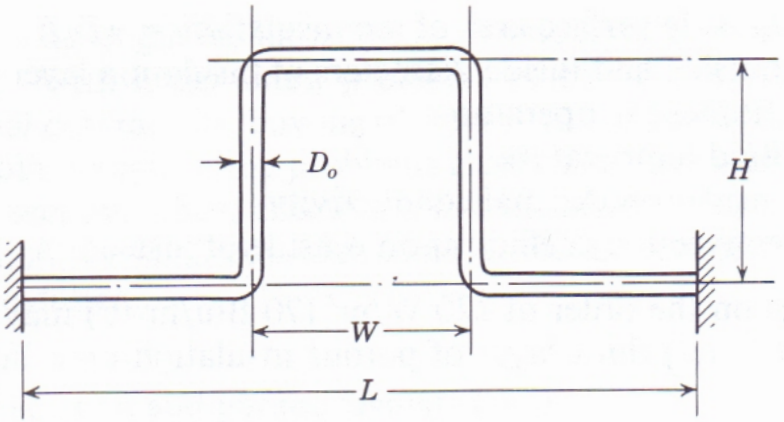

Fig. 7.20. U-bend in a cryogenic-fluid transfer line. It is assumed that the ends are rigidly connected to supports (the worst case for thermal-contraction effects).

7.17 Vacuum-insulated lines

If the outside diameter is much smaller than the length of the line, elastic-energy theory may be applied to determine the maximum thermal stress.

1) $\alpha = W/L \geq 1/2$:

$$\frac{\sigma\_\max L}{E e_t D_0} = \frac{\alpha+\beta}{B}\left[1+\frac{(1+2\beta)D_0}{4(\alpha+\beta)H}\right]$$

2) $\alpha < 1/2$:

$$\frac{\sigma\_\max L}{E e_t D_0} = \frac{1-\alpha+\beta}{B}\left[1+\frac{(1+2\beta)D_0}{4(1-\alpha+\beta)H}\right]$$

$$B = \frac{2}{3}\beta\left[\beta(2+\beta)+3\alpha(1-\alpha)+\frac{3}{8}(1+2\beta)\left(\frac{D_0}{H}\right)^2\right]$$

$$\alpha = \frac{W}{L}(optimum\ value = 0.5), \beta = \frac{H}{L}$$

$$e_t = \int_{T_c}^{T_h} \lambda dT = unit\ thermal\ strain$$

7.17 Vacuum-insulated lines

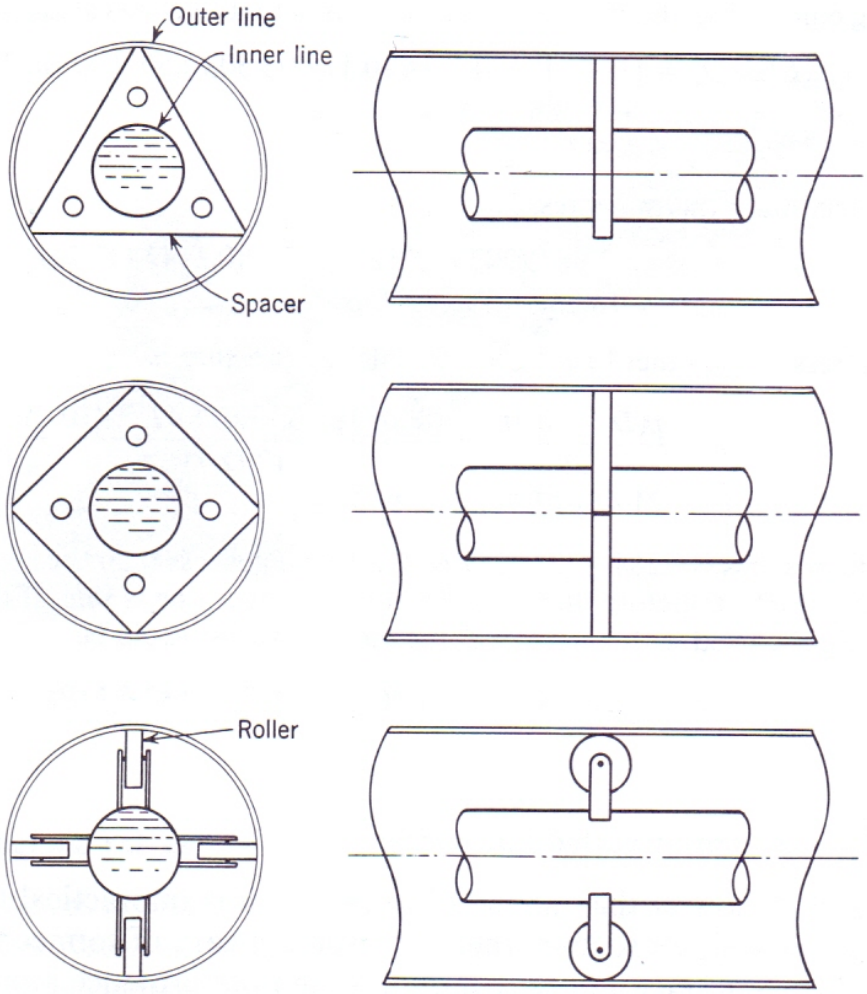

Fig. 7.21. Typical spacers used to separate the inner and outer lines in a vacuum-jacketed cryogenic-fluid transfer line.

7.18 Vacuum-insulated line joints

For lengths longer than about 12m,
it is impractical to construct the line in a single section.

A high-performance joint, called **the bayonet joint**,
developed by Dr. Herrick L. Johnston, is used frequently.

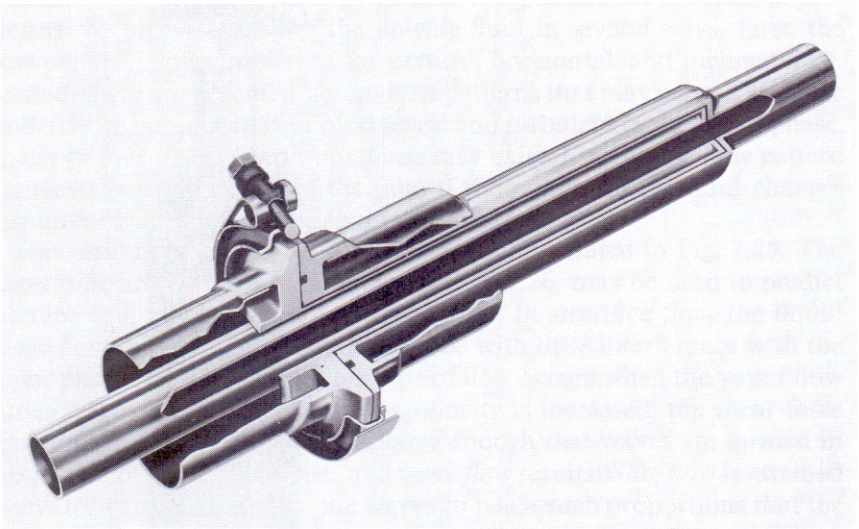

Fig. 7.22. Bayonet joint for vacuum-jacketed transfer lines (CVI Corp., Columbus, Ohio).

It consists of a male portion that telescopes within the female portion.
The clearance between two portions is made such that
no liquid can flow into the space, and gaseous convection is suppressed.
The neoprene O-ring is sealed in the warm flange.
For ease and speed in assembly, a V-band clamp is used to hold the two portion.

7.18 Vacuum-insulated line joints

For application in which the line is seldom taken apart once it is installed,
the field-welded joint is frequently used.
The line section are welded together at the site,
and the outer casing on the joint is welded in place.
The space between the inner-line weld and the joint sleeve
is finally evacuated and sealed off.

Fig. 7.23. Field-welded joint assembly for vacuum-jacketed transfer lines (CVI Corp., Columbus, Ohio).

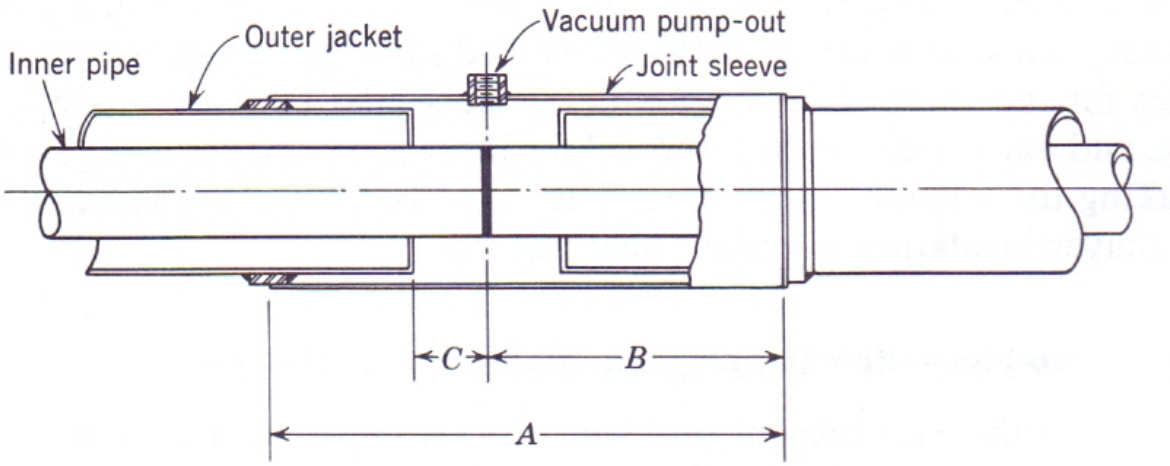

7.19 Cryogenic valves

- **Cryogenic valves**
  - Extended-stem valve
  - Vacuum-jacketed valve

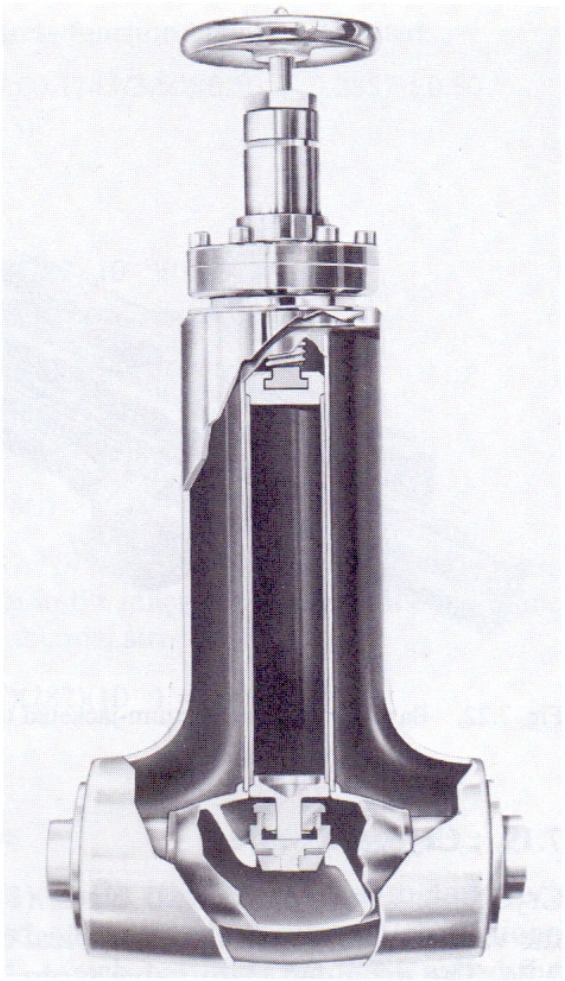

Fig. 7.24. Vacuum-jacketed cryogenic valve (CVI Corp., Columbus, Ohio).

7.19 Cryogenic valves

- **Extended-stem valve**

  Resembles an ordinary valve, except that the valve stem is modified by extending the stem about 250 mm to 300 mm through the use of thin-walled tubing

  - Advantages

    - The valve handle is maintained at ambient temperature to protect the operator
    - The valve stem may be sealed at ambient temperature thereby eliminating a severe sealing problem and improving the reliability

7.19 Cryogenic valves

- **Vacuum-jacketed valve**

  An extended-stem valve with a vacuum jacket around the extended stem and valve body to reduce heat inleak

  - Advantages

    - Valve stem, valve plug, and valve seal can be removed for inspection
    - The valve body is insulated with multilayer insulation to reduce heat transfer

7.20 Two-phase flow in cryogenic-fluid transfer systems

- **Two-phase flow problem**

  Two-phase flow complicates the problem of predicting the pressure drop of the flowing fluid in several ways.

  - The flow pattern is often different for vertical, horizontal, and inclined flow.
  - Several different flow patterns exist
  - The flow may be laminar in the liquid phase and turbulent in the vapor phase or any of four different combinations exist
  - The flow pattern changes along the length of the pipe if the quality of the fluid changes because of heat transfer or pressure drop (flashing)

7.20 Two-phase flow in cryogenic-fluid transfer systems

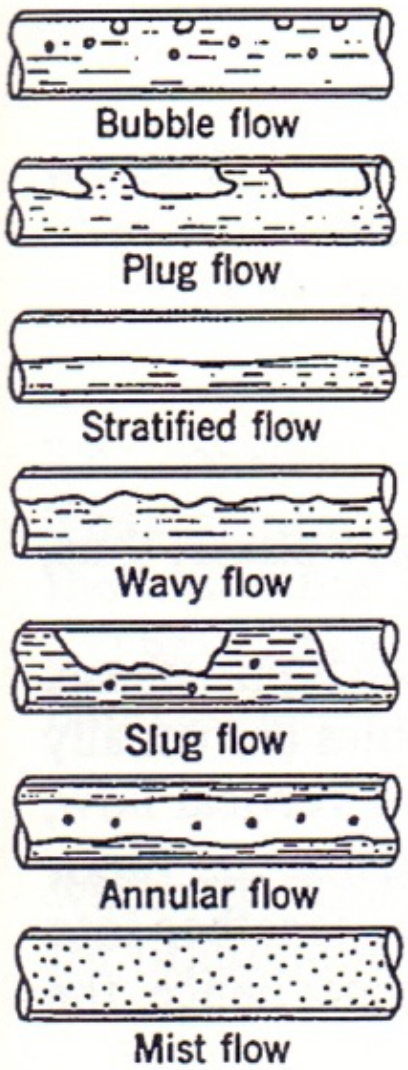

Fig. 7.25. Two-phase flow patterns for horizontal flow.

7.20 Two-phase flow in cryogenic-fluid transfer systems

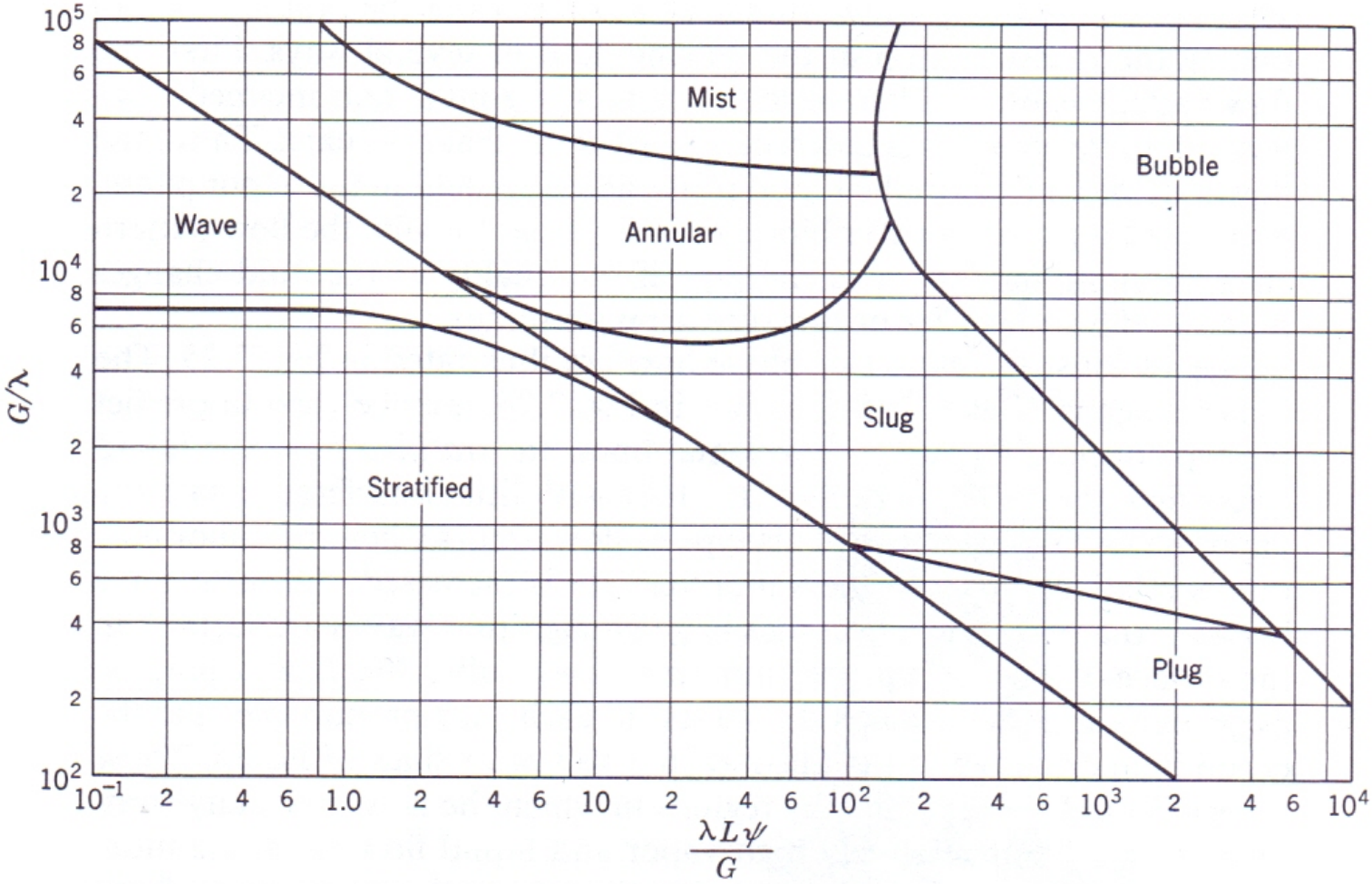

Fig. 7.26. Two-phase flow pattern regions according to Baker (1954).

7.21 Pressure drop in two-phase flow

- **Lockhart-Martinelli correlation**

$$(\Delta p/\Delta L)_{TP} = \phi_L^2 (\Delta p/\Delta L)_L \qquad (7.56)$$

$$X^2 = \frac{(\Delta p/\Delta L)_L}{(\Delta p/\Delta L)_G} = \frac{C_L(\mathrm{Re}_G)^m \rho_G}{C_G(\mathrm{Re}_L)^n \rho_L} \left(\frac{1-x}{x}\right)^2 \qquad (7.57)$$

$(\Delta p/\Delta L)_{TP}$: pressure drop per unit length for two-phase flow

$(\Delta p/\Delta L)_L$: pressure drop per unit length for liquid flow

$(\Delta p/\Delta L)_G$: pressure drop per unit length for vapor flow

$$\mathrm{Re}_L = D\dot{m}_L/A\mu_L \quad \text{and} \quad \mathrm{Re}_G = D\dot{m}_G/A\mu_G \qquad (7.58)$$

where D = tube inside diameter
μ = viscosity
A = cross-sectional area of tube
$\dot{m}$ = mass flow rate

and,

7.21 Pressure drop in two-phase flow

- **Lockhart-Martinelli correlation**

$$\mathrm{Re}_L = D\dot{m}_L/A\mu_L \quad \text{and} \quad \mathrm{Re}_G = D\dot{m}_G/A\mu_G \tag{7.58}$$

where D = tube inside diameter
μ = viscosity
A = cross-sectional area of tube
$\dot{m}$ = mass flow rate

and,

Table 7.19. Lockhart-Martinelli correlation constants

Constant	Laminar	Turbulent	
	Re < 2000	3000 < Re < 50 000	Re > 50 000
m (vapor)	1	0.25	0.20
n (liquid)	1	0.25	0.20
C_G (vapor)	64	0.316	0.184
C_L (liquid)	64	0.316	0.184

The four possible combinations are:
vv = laminar liquid, laminar vapor
vt = laminar liquid, turublent vapor
tv = turbulent liquid, laminar vapor
tt = turbulent liquid, turbulent vapor

7.21 Pressure drop in two-phase flow

- **Lockhart-Martinelli correlation**

$$\phi_L = (X^2 + CX + 1)^{1/2}/X \qquad (7.59)$$

Liquid	Vapor	C
Laminar	Laminar (vv)	5
Turbulent	Laminar (tv)	10
Laminar	Turbulent (vt)	12
Turbulent	Turbulent (tt)	20

$$(\Delta p/\Delta L)_L = f(\dot{m}_L/A)^2/2g_c\rho_L D \qquad (7.60)$$

7.22 The cool-down process

- **Cool down process**

As the fluid enters the line, which is initially at ambient temperature, the liquid is quickly boiled in cooling the transfer-line mass near the tube entrance.

We can analyze the cool-down process by considering Fig. 7.27.

Fig. 7.27. Thermodynamic system used in transfer-line cool-down analysis. The system consists of the space within the inner line.